Geological Survey of Japan Cruise Report No. 20, p. 242–262, 1984

XV. LOCAL VARIABILITY OF MANGANESE NODULE CHEMISTRY AND ITS RELATIONSHIP TO MINERALOGY IN THE GH80–5 AREA

Akira Usui and Tsunekazu Mochizuki

Introduction

Compositional variation of manganese nodules on various scales are of economic and scientific interests. Earlier investigations in nodule chemistry have revealed significant regional variation in the Pacific and Indian Oceans, and found several abundant and high-grade nodule provinces (HORN *et al.*, 1972; FRAZER and WILSON, 1979). During the recent detailed investigations, local small-scale variability in nodule morphology and chemistry has been also found (ANDREWS and FRIEDRICH, 1979; HALBACH and ÖZKARA, 1979; MIZUNO, 1981). However, the patterns of variations in nodule morphology, bulk chemistry and mineralogy on the small scales have not been perfectly understood. In the GH80–5 area, variation patterns of nodule physical characteristics were well defined on the basis of on-site observations, in-laboratory mineralogical analyses (USUI, Chapter IX in this cruise report; USUI Chapter XIV in this cruise report). This article demonstrates the relationships of chemical composition to mineral composition and microstructure based on the quantitative mineral and chemical analysis.

Samples

Chemical analyses were made on one hundred and forty five powder samples taken from defined parts of manganese nodules. The analyzed parts were prescribed according to external and internal morphology; samples from nodule tops, bottoms, outer layer, inner parts, and entire nodules were prepared. This description of analysed parts proved important in understanding the relationship between mineral and chemical compositions as compared with previous bulk analyses. More than one samples were selected from each station as representatives of the stations.

All analysis data of chemical and mineral compositions are recorded on diskette files and processed using a personal computer. Analysis numbers are common to those in Table XIV–3 (USUI, Chapter XIV in this cruise report).

Analytical methods

Air-dried samples were ground into powder under 100 mesh. The powder samples were subjected to X-ray diffraction semi-quantitative analysis (USUI, Chapter XIV in this cruise report), and 0.1 g of them were prepared for chemical analysis. The samples were melt with sodium carbonate and boric acid, and the fusion was

dissolved with dilute (1:9) hydrochloric acid. Lanthanum chloride was added to the solution to prevent the interference of other components. Mn, Fe, Cu, Ni, Co, Si and Al were determined by atomic absorption spectroscopy. Water contents were determined as H_2O+ and H_2O-, by the Penfield Method and by drying in ovens at 110°C 3 hours, respectively. Details of analytical technique and procedure have been reported by FUJINUKI *et al.* (1977) and TERASHIMA (1978).

Results and discussion

Concentrations of seven metal elements and water contents (H_2O+) normalized to 110°C dried powder samples are listed in Table XV–1 with nodule morphology and analyzed parts. The water content (H_2O-) is loss of heating at 110°C normalized to air-dried samples.

When converted to oxides (MnO_2, Co_2O_3 etc.) the analyses of nodules sum to between 67 to 91 wt.% with the average of 83 wt.%. The nodules of the GH80–5 area are characteristic of a great differentiation in chemical composition, as most distinctly represented by Mn/Fe ratio. The ratio shows more than 10-fold variation ranging from 0.88 to 10.9. This range is comparable to or even greater than that of regional variations for nodules in the world oceans. It must be noted that the samples for analyses were taken from restricted parts therefore they do not represent the bulk chemical characteristics of nodules. Variations of nodule composition are expected to be smaller if all analyses were made on entire nodule samples.

Nodule morphology and chemical composition

RAAB (1972) has first noted that chemical compositions are occasionally different between nodule tops and bottoms when their surface morphology is different.

The data of chemical compositions of GH80–5 area show significant differences with analyzed parts of nodules (Table XV–2. Bottom rough surfaces and entirely rough-surface nodules are very similar in composition. Top smooth surfaces and internal older nodules which often occur with rough-surface nodules are similar in composition. Significant compositional differences are recognized between the two groups. The differences are most distinct in Cu plus Ni and Fe concentrations. Rough-surface nodules (Types r and s·r+r: see in Figure IV–1) and bottom gritty surfaces of smooth-surface nodule (s+r and s+s·r) are enriched in Cu and Ni and depleted in Fe, while smooth surfaces are, in contrast, enriched in Fe and depleted in Cu and Ni.

These chemical features in relation to morphology are in good accordance with mineral composition. USUI *et al.* (1978) concluded with microscopical and microprobe analyses that gritty surface is composed of the 10 Å manganate phase and smooth surface of the δ–MnO_2 phase. The results of comparative study of chemistry and mineralogy on GH80–5 nodules strongly support this interpretation. Samples of high Cu, Ni and Mn and low Fe encountered in rough surface nodules and gritty bottoms of smooth surface nodules are always enriched in 10 Å manganate. On the other hand, samples of high Fe and low Cu, Ni and Mn are enriched in δ–MnO_2. Samples of outer layers of surrounding older nodules are slightly biased to 10 Å manganate feature, which is also well agreeable to the mineralogical study that the layers are often composed of alternated layers of the 10 Å manganate and δ–MnO_2

Table XV-1 Chemical composition and morphology of manganese nodules. H−: H_2O-, H+: H_2O+. H_2O- is normalyzed to air-dried samples, whereas the others are normalyzed to 110°C dried samples. O: outer part, I: inner part, W: whole nodule, T: top, B: bottom, X: unspecified part

Analysis	Station	Sample	Nodule sample			Chemical composition(%)									
No.	No.	No.	Shape	Surface	Part	Mn	Fe	Cu	Ni	Co	Si	Al	H+	H−	Mn/Fe
1	1979	F252-1	IS	1	O(0-3)	14.76	16.84	0.28	0.21	0.38	5.26	1.59	14.53	21.57	0.88
2					I	24.87	14.65	0.45	0.66	0.42	5.26	2.17	9.55	24.62	1.70
3	1983	F256-1	D	3	W	25.36	11.28	0.79	0.84	0.28	6.99	3.52	8.84	21.73	2.25
4		F256-2	D	3	T(0-2)	22.52	17.75	0.28	0.48	0.40	5.64	2.09	9.93	24.08	1.27
5					B(0-1)	28.22	6.46	1.14	1.46	0.14	7.33	3.70	6.87	19.91	4.37
6	1984	B34	S	6	W(0-7)	24.94	6.91	1.09	1.11	0.22	7.96	3.79	10.55	20.24	3.61
7		F257	S	6	W(0-7)	27.93	6.94	1.24	1.17	0.23	7.32	3.71	9.35	18.65	4.02
8	1985	F258-1	S	6	W(0-10)	27.31	7.36	1.09	1.18	0.21	7.81	3.62	8.78	19.67	3.71
9	1988	F261-1	S	1	O(0-3)	21.86	18.21	0.23	0.37	0.42	6.11	2.00	9.76	24.62	1.20
10					I	20.57	15.07	0.26	0.34	0.33	6.51	2.72	8.68	24.36	1.36
11		F261-2	D	1	W	20.87	14.32	0.40	0.45	0.33	5.35	2.26	11.00	22.87	1.46
12	1989	B36	D	1	W	22.24	14.90	0.42	0.49	0.36	6.41	2.48	10.33	23.16	1.49
13	1990	F263-1	D	1	W	23.03	15.56	0.40	0.56	0.33	5.28	1.93	10.48	23.40	1.48
14	1991	B37	DP	1	W	22.91	14.82	0.36	0.54	0.37	6.15	2.29	10.66	22.53	1.55
15	1987	B35	S	6	W(0-10)	24.56	7.46	1.00	1.02	0.22	7.62	3.38	9.43	18.74	3.29
16		F260	S	6	W(0-10)	26.10	7.06	1.09	1.05	0.19	6.68	3.29	10.10	18.07	3.70
17	1992	F267	S	6	W(0-10)	26.90	5.70	1.14	1.15	0.17	6.58	3.16	9.12	17.99	4.72
18	1993	F268	S	6	W(0-10)	27.36	5.26	1.27	1.14	0.14	6.79	3.26	9.40	16.96	5.20
19	1994	B38	S	6	W(0-10)	25.44	5.14	1.16	1.04	0.14	7.52	3.27	8.33	17.68	4.95
20	1995	F269	S	6	W(0-10)	25.99	5.33	1.19	1.14	0.15	6.23	3.14	9.68	17.27	4.88
21	1996	F270	ISP	3	T(0-1)	17.06	13.77	0.36	0.41	0.29	9.68	3.41	—	17.90	1.24
22					B(0-2)	20.47	8.95	0.58	0.96	0.19	9.64	3.93	10.57	17.62	2.29
23	1997	F271	S	6	W(0-10)	25.22	6.39	1.14	1.08	0.17	6.27	3.38	10.82	16.50	3.95
24	1998	B39	S	4	W	25.80	7.22	1.10	1.13	0.21	6.35	3.46	10.86	17.53	3.57
25			D	4	W	24.79	8.32	0.89	0.94	0.20	5.79	3.02	11.02	17.71	2.98
26	1999	F272	IS	2	T(0-2)	20.80	16.33	0.28	0.44	0.33	5.28	2.07	10.69	21.83	1.27
27					I	16.83	11.10	0.27	0.36	0.22	7.01	3.23	11.33	20.75	1.52
28					B(0-1)	24.98	12.02	0.79	0.85	0.26	5.29	2.37	11.19	20.57	2.08

Table XV-1 (continued)

Analysis	Station	Sample	Nodule sample			Chemical composition(%)									
No.	No.	No.	Shape	Surface	Part	Mn	Fe	Cu	Ni	Co	Si	Al	H+	H-	Mn/Fe
29	1986	P196	ID	2	T(0-2)	21.37	16.49	0.25	0.44	0.37	5.50	1.98	11.30	22.06	1.30
30		F259-1	IDP	2	T(0-2)	20.29	16.93	0.16	0.40	0.33	5.12	1.91	11.55	22.57	1.20
31					I	19.46	12.24	0.34	0.42	0.22	8.80	4.08	10.93	20.65	1.59
32					B(0-2)	24.21	9.46	0.82	0.92	0.22	5.17	2.63	10.75	20.30	2.56
33	1982	F255-2	D	2	T(0-2)	24.62	11.27	0.67	1.02	0.26	4.24	2.02	10.42	21.63	2.18
34					I	20.59	14.17	0.26	0.37	0.61	5.20	2.14	10.78	23.72	1.45
35	2000	F273	DP	1	T(0-2)	22.36	12.94	0.49	0.60	0.31	5.29	2.47	11.80	23.59	1.73
36					I	19.44	16.08	0.34	0.48	0.36	5.20	1.93	10.35	23.75	1.21
37	2001	F274	ID	1	O(0-2)	18.96	13.70	0.21	0.34	0.29	5.34	2.12	10.99	22.72	1.38
38					I	19.99	16.88	0.15	0.30	0.38	4.08	1.29	10.59	22.21	1.18
39	2002	F275	ISP	1	O(0-3)	20.11	18.65	0.29	0.39	0.32	6.90	2.31	10.93	23.19	1.08
40					I	19.57	15.14	0.32	0.40	0.23	8.60	3.34	10.30	21.89	1.25
41	2003	B40	ISP	3	T(0-2)	22.03	17.09	0.26	0.49	0.35	6.31	2.01	11.41	21.75	1.29
42					I	21.93	13.78	0.39	0.47	0.27	7.95	3.39	11.84	22.23	1.59
43					B(0-1)	33.32	4.52	1.58	1.52	0.18	5.45	2.28	—	19.96	7.37
44	2004	F276	SP	3	T(0-2)	21.75	15.67	0.40	0.55	0.30	7.11	2.62	11.85	20.82	1.39
45					I	24.68	8.21	0.97	0.96	0.20	7.47	3.93	12.32	17.18	3.01
46					B(0-1)	22.85	13.60	0.61	0.69	0.22	7.00	2.89	11.91	20.67	1.68
47	2005	F277	S	6	W(0-5)	23.00	6.66	1.04	1.11	0.19	8.28	4.18	11.41	16.93	3.45
48			D	6	O(0-2)	21.90	10.49	0.62	0.74	0.19	6.14	2.51	11.68	19.64	2.09
49					I(2-10)	19.00	7.37	0.72	0.58	0.14	11.51	5.16	9.52	15.83	2.58
50	2006	P199	S	6	W	26.02	4.95	1.18	1.18	0.15	6.81	3.34	10.91	16.50	5.26
51	2007	F278	S	6	O(0-10)	26.72	5.77	1.27	1.17	0.15	6.84	3.17	10.51	16.86	4.63
52					I	25.61	4.54	1.41	1.20	0.13	6.17	4.33	—	13.97	5.64
53	1981	B33	S	6	O(0-15)	23.89	5.46	1.02	1.05	0.14	6.81	3.19	9.95	17.44	4.38
54					I	26.35	4.47	1.45	1.18	0.17	6.62	4.12	10.79	15.00	5.89
55		F254	S	6	W(0-10)	26.09	5.30	1.21	1.16	0.15	6.88	3.34	10.72	16.53	4.92
56	2008	F279	S	6	W(0-15)	25.89	7.17	1.09	1.06	0.16	7.58	3.76	10.68	17.64	3.61
57	2009	F280	D	6	W(0-20)	27.37	5.73	1.26	1.09	0.13	6.63	3.29	10.75	16.25	4.78

Table XV-1 (continued)

Analysis No.	Station No.	Sample No.	Nodule sample			Chemical composition(%)									
			Shape	Surface	Part	Mn	Fe	Cu	Ni	Co	Si	Al	H+	H-	Mn/Fe
58	2010	F281	S	6	W(0-5)	26.34	5.29	1.15	1.19	0.15	7.47	3.56	10.55	16.35	4.98
59	2011	F281	D	6	W(0-20)	28.92	5.56	1.32	1.08	0.14	6.12	3.19	10.56	16.40	5.20
60		F285	D	4	O(0-2)	21.02	9.19	0.62	0.73	0.18	6.29	2.66	9.94	19.67	2.29
61					I	24.78	6.63	1.23	1.00	0.18	6.13	3.75	11.16	17.54	3.74
62	2012	F282	S	6	W(0-4)	26.68	4.08	1.16	1.18	0.13	6.83	3.26	10.48	16.73	6.54
63	2013	F283	S	6	W(0-10)	28.79	4.11	1.22	1.24	0.14	6.23	3.03	9.80	17.30	7.00
64				6	W(0-20)	25.70	5.78	1.18	1.03	0.13	6.09	3.08	10.28	17.08	4.45
65	2014	B41	D	5	O(0-1)	27.54	3.61	1.14	1.17	0.13	6.70	2.81	—	16.09	7.63
66					I	20.51	8.39	0.76	0.67	0.17	7.67	4.23	10.70	18.55	2.44
67	2015	F284	IDP	2	O(0-2)	20.55	12.21	0.53	0.68	0.24	5.55	2.36	11.41	21.35	1.68
68					I	17.69	9.19	0.55	0.55	0.17	6.69	3.47	11.18	19.63	1.92
69	1980	F-253-1	IDP	3	T(0-2)	20.75	16.97	0.18	0.38	0.26	4.84	1.74	10.74	23.78	1.22
70					I	24.77	9.94	0.91	0.90	0.24	5.73	3.41	11.41	18.24	2.49
71					B(0-1)	29.09	3.67	1.41	1.53	0.13	4.65	2.63	9.97	17.51	7.93
72	2019	B43	S	6	W	27.51	5.60	0.98	0.89	0.18	6.44	2.45	9.34	17.63	4.91
73	2020	B44	D	6	W	26.27	5.45	1.15	1.16	0.14	6.15	2.94	9.48	18.81	4.82
74		F289	D	6	O(0-3)	25.85	6.85	1.11	1.17	0.17	6.18	3.10	10.21	19.21	3.77
75					I(3-8)	8.63	6.56	0.29	0.21	0.08	16.68	6.72	—	15.65	1.32
76	2023	F292	I	6	W	22.39	8.84	0.74	0.75	0.20	7.48	2.97	9.94	20.59	2.53
77	2024	F293	ID	6	O(0-2)	29.72	2.73	1.18	1.10	0.23	5.57	2.11	—	19.27	10.89
78					I	18.57	12.05	0.39	0.37	0.23	4.89	2.06	11.42	23.44	1.54
79	2025	F294	I	6	W	22.07	6.75	0.80	0.90	0.12	8.60	3.24	9.16	19.46	3.27
80	2028	F297-2	IS	1	O(0-2)	19.75	12.80	0.43	0.52	0.28	5.73	2.25	11.30	22.08	1.54
81					I	14.06	15.37	0.21	0.23	0.15	8.84	3.43	9.27	22.34	0.91
82	2021	F290-1	D	6	W	25.65	5.72	1.14	1.09	0.12	6.80	2.94	8.58	19.08	4.46
83		F290-2	S	6	W	27.48	6.42	1.25	1.20	0.14	7.06	3.06	9.15	18.80	4.28
84	2041	F304	SP	6	O(0-2)	24.43	7.49	0.87	1.03	0.17	6.92	2.57	9.08	20.39	3.26
85					I	17.79	7.16	1.13	0.84	0.21	9.69	4.90	9.51	16.16	2.48
86	2042	B55	S	6	W	26.85	6.19	1.18	1.12	0.18	6.62	3.15	—	19.12	4.34
87	2043	F305	D	6	W	23.70	6.41	1.07	1.03	0.14	5.67	2.86	9.95	18.97	3.70

Table XV-1 (continued)

Analysis No.	Station No.	Sample No.	Nodule sample			Chemical composition									
			Shape	Surface	Part	Mn	Fe	Cu	Ni	Co	Si	Al	H+	H-	Mn/Fe
88	2044	B56	ID	5	O(0-1)	27.23	5.68	1.02	1.02	0.25	6.39	2.20	8.54	20.26	4.79
89					I	15.22	8.74	0.37	0.37	0.15	9.63	4.07	9.42	20.83	1.74
90	2046	F307	IDP	5	T(0-2)	19.61	13.51	0.28	0.45	0.25	5.67	1.95	10.51	22.31	1.45
91					I	19.91	8.75	0.69	0.67	0.19	8.93	3.94	12.40	18.19	2.28
92					B(0-1)	30.61	6.02	0.98	1.29	0.20	5.03	2.09	—	21.63	5.08
93		P206	ID	4	O(0-3)	22.58	13.63	0.45	0.59	0.29	6.24	2.23	12.50	21.26	1.66
94					I	19.07	12.62	0.30	0.37	0.23	7.24	2.62	11.61	21.77	1.51
95	2045	F306	IS	2	T(0-1)	27.05	9.36	0.84	1.08	0.27	4.29	2.00	11.42	19.50	2.89
96					I	20.33	12.40	0.39	0.45	0.26	6.67	2.62	12.74	20.78	1.64
97					B(0-1)	23.80	13.11	0.54	0.69	0.29	5.99	2.13	11.85	21.79	1.82
98	2022	B45	ID	2	T(0-3)	21.20	15.97	0.23	0.38	0.32	5.60	1.62	12.51	22.34	1.33
99					I	19.39	14.07	0.37	0.49	0.22	7.50	2.76	11.70	19.43	1.38
100					B(0-1)	25.84	7.95	0.90	1.06	0.19	5.05	2.08	—	21.48	3.25
101		F291	ID	2	O(0-2)	21.88	14.91	0.32	0.48	0.32	5.73	2.09	11.77	23.15	1.47
102					I	21.02	14.07	0.29	0.40	0.30	6.03	2.28	13.09	21.65	1.49
103	2026	F295-2	D	6	O(0-2)	24.96	8.46	0.90	1.06	0.19	6.16	2.87	11.89	18.23	2.95
104					I	18.28	7.10	0.78	0.66	0.19	7.34	3.95	12.35	18.40	2.57
105		F295-1	S	6	O(0-2)	26.18	6.43	1.09	1.08	0.15	5.77	2.83	11.50	17.05	4.07
106					I(2-10)	20.82	8.68	0.76	0.61	0.19	6.67	3.14	12.40	19.76	2.40
107	2034	B51	D	6	O(0-1)	31.65	3.50	1.27	1.24	0.17	5.67	2.24	10.07	18.93	9.04
108					I	24.11	5.77	1.04	1.05	0.14	6.09	2.91	11.41	17.36	4.18
109	2033	F300	S	6	O(0-10)	28.18	4.55	1.08	1.17	0.14	6.16	2.47	10.46	18.29	6.19
110					X(10-20)	27.46	4.55	1.30	1.30	0.13	5.78	2.96	10.86	16.16	6.04
111					I(20-40)	15.90	12.05	0.30	0.26	0.16	8.63	3.23	11.74	20.45	1.32
112	2032	B50	SP	6	O(0-1)	29.44	3.76	1.20	1.27	0.16	5.13	2.17	10.86	18.93	7.83
113					X(1-10)	25.17	8.82	0.83	0.99	0.19	5.78	2.37	12.01	18.26	2.85
114					I(10-40)	14.64	11.78	0.28	0.24	0.16	6.82	2.46	11.87	21.43	1.24
115	2031	F299	IS	2	O(0-3)	24.36	9.80	0.94	1.00	0.19	5.14	2.32	11.42	19.19	2.49
116					I	13.62	12.28	0.22	0.22	0.15	8.30	2.64	12.12	20.30	1.11

Table XV-1 (continued)

Analysis No.	Station No.	Sample No.	Nodule sample			Chemical composition									
			Shape	Surface	Part	Mn	Fe	Cu	Ni	Co	Si	Al	H+	H-	Mn/Fe
117	2030	B49	ID	2	B(0-1)	30.83	3.41	1.33	1.23	0.17	4.67	1.71	—	19.17	9.04
118					T	21.02	11.72	0.51	0.41	0.22	5.62	2.06	11.83	20.52	1.79
119					I	22.75	15.36	0.39	0.44	0.30	5.47	2.01	—	22.17	1.48
120	2029	F298	ID	2	T(0-2)	20.56	16.72	0.32	0.43	0.27	5.67	1.95	11.90	22.23	1.23
121					I	19.46	15.18	0.24	0.32	0.28	5.26	2.21	12.05	23.30	1.28
122					B(0-1)	23.38	11.36	0.58	0.82	0.25	5.42	2.39	11.50	21.43	2.06
123	2027	F296	ID	4	O(0-1)	22.50	11.08	0.65	0.80	0.27	5.40	2.45	11.43	20.14	2.03
124					I	22.95	17.11	0.18	0.29	0.33	3.40	1.33	12.01	25.16	1.34
125			C	1	W(0-5)	20.73	19.35	0.15	0.29	0.34	3.80	1.48	11.71	24.14	1.07
126		B48	IDP	1	O(0-2)	22.81	13.89	0.49	0.77	0.27	5.86	2.32	11.90	21.22	1.64
127					I	15.39	11.49	0.24	0.29	0.19	5.40	2.15	—	22.33	1.34
128	2018	F287-2	S	6	W(0-10)	32.68	3.50	0.92	0.91	0.18	5.31	1.86	9.58	17.09	9.34
129		F287-1	SP	6	W	29.08	4.66	0.92	0.98	0.14	5.99	2.27	9.43	17.75	6.24
130	2040	B54	S	6	W	25.29	5.54	0.82	0.79	0.18	7.07	2.58	9.15	17.46	4.56
131	2039	F303	S	6	W(0-7)	32.37	4.12	1.02	1.02	0.18	5.88	2.26	9.41	17.30	7.86
132	2038	B53	S	6	W(0-7)	27.84	3.83	0.84	0.78	0.18	4.76	1.71	9.49	17.18	7.27
133	2037	F302	S	6	W(0-12)	24.32	5.35	0.98	1.07	0.13	5.96	2.90	10.19	17.40	4.55
134	2036	B52	IS	6	O(0-1)	27.71	2.84	1.23	1.60	0.10	5.85	3.17	9.74	17.99	9.76
135					X(1-5)	21.23	10.70	0.74	0.74	0.26	6.34	3.04	11.03	19.44	1.98
136					X(5-15)	18.63	13.26	0.45	0.33	0.24	6.84	3.00	11.24	22.71	1.40
137					I(15-30)	17.19	16.10	0.25	0.19	0.21	7.52	2.62	10.08	22.38	1.07
138	2035	F301	ID	4	O(0-3)	24.04	10.25	0.80	1.03	0.22	5.68	2.70	10.96	19.72	2.35
139					I	19.69	13.29	0.31	0.32	0.26	4.57	2.02	11.54	23.50	1.48
140	2017	F286	ID	3	T(0-4)	18.06	13.01	0.21	0.39	0.24	4.62	1.85	11.07	22.45	1.39
141					I	13.74	12.47	0.20	0.15	0.17	5.70	2.18	10.55	22.15	1.10
142					B(0-1)	24.63	2.80	1.15	1.20	0.08	4.67	2.57	10.76	16.83	8.80
143		B42	ID	3	T(0-3)	22.01	15.22	0.31	0.59	0.27	5.35	2.13	12.52	20.48	1.45
144					I	16.61	15.99	0.27	0.23	0.18	7.63	3.53	12.01	20.41	1.04
145					B(0-1)	29.03	3.75	1.26	1.28	0.12	4.92	2.52	—	18.51	7.74

Table XV-2 Difference of chemical and mineral compositions with analyzed parts of nodules

Type: all				n=145									
Part: all													
	Mn	Fe	Cu	Ni	Co	Si	Al	H+	H−	T	D	Q	Ph	Pc
Mean	23.16	9.82	0.73	0.78	0.23	6.41	2.79	10.7	19.9	31.0	6.9	24.0	1.7	0.6
S. D.	4.27	4.46	0.39	0.36	0.08	1.54	0.80	1.1	2.4	23.3	4.3	7.8	2.6	1.8
Max.	33.32	19.35	1.58	1.60	0.61	16.68	6.72	14.5	25.2	86.0	16.0	66.0	15.0	13.0
Min.	8.63	2.73	0.15	0.19	0.08	3.4	1.29	6.9	14.0	0.0	4.5	6.0	0.0	0.0
Type: r				n=34									
Part: entire													
	Mn	Fe	Cu	Ni	Co	Si	Al	H+	H−	T	D	Q	Ph	Pc
Mean	26.47	5.78	1.09	1.06	0.16	6.75	3.09	9.8	17.8	53.2	3.1	29.7	1.3	0.2
S. D.	2.29	1.16	0.14	0.13	0.03	0.84	0.53	0.7	1.2	8.9	2.6	5.6	1.6	0.7
Max.	32.68	8.84	1.32	1.24	0.23	8.60	4.18	11.4	20.6	78.0	8.2	47.0	6.0	3.0
Min.	22.07	3.50	0.74	0.75	0.12	4.76	1.71	8.3	16.3	36.0	4.5	17.0	0.0	0.0
Type: s+s·r, s+r				n=13									
Part: bottom													
	Mn	Fe	Cu	Ni	Co	Si	Al	H+	H−	T	D	Q	Ph	Pc
Mean	26.20	7.77	0.98	1.09	0.19	5.79	2.60	10.6	19.7	45.7	4.4	23.9	0.5	0.0
S. D.	3.63	3.94	0.36	0.30	0.06	1.43	0.62	1.5	1.6	21.3	3.7	4.6	1.6	0.0
Max.	33.32	13.60	1.58	1.53	0.29	9.64	3.93	11.9	21.8	77.0	8.7	32.0	6.0	0.0
Min.	20.47	2.80	0.54	0.69	0.08	4.65	1.71	6.9	16.8	20.0	1.2	14.0	0.0	0.0
Type: s, s+s·r, s+r				n=16									
part: top													
	Mn	Fe	Cu	Ni	Co	Si	Al	H+	H−	T	D	Q	Ph	Pc
Mean	21.46	14.82	0.36	0.53	0.30	5.64	2.12	11.4	21.7	14.5	9.3	21.1	0.6	0.0
S. D.	2.28	2.49	0.19	0.21	0.05	1.29	0.42	7.3	1.6	8.5	1.7	5.2	1.9	0.0
Max.	27.05	17.75	0.84	1.08	0.40	9.68	3.41	12.5	24.1	34.0	13.0	32.0	8.0	0.0
Min.	17.06	9.36	0.16	0.38	0.22	4.24	1.62	9.9	17.9	4.0	6.0	11.0	0.0	0.0
Type: s, s+s·r				n=9									
Part: outermost													
	Mn	Fe	Cu	Ni	Co	Si	Al	H+	H−	T	D	Q	Ph	Pc
Mean	20.56	14.55	0.41	0.53	0.30	5.74	2.15	11.5	22.1	15.4	8.6	20.5	0.0	0.0
S. D.	2.73	2.91	0.23	0.25	0.07	0.53	0.24	1.3	1.6	9.7	2.0	4.5	0.0	0.0
Max.	24.36	18.65	0.94	1.00	0.42	6.90	2.36	14.5	24.6	33.0	12.0	27.0	0.0	0.0
Min.	14.76	9.80	0.21	0.21	0.19	5.14	1.59	9.8	19.2	4.0	4.7	11.0	0.0	0.0
Type: s, s+s·r				n=17									
Part: innermost													
	Mn	Fe	Cu	Ni	Co	Si	Al	H+	H−	T	D	Q	Ph	Pc
Mean	19.11	13.80	0.31	0.40	0.28	6.52	2.62	11.0	22.1	4.4	11.8	16.5	2.8	1.4
S. D.	2.89	2.03	0.10	0.11	0.12	1.47	0.71	1.3	1.6	5.3	1.3	4.4	2.3	2.0
Max.	24.87	16.88	0.55	0.66	0.61	8.84	4.08	13.1	24.6	20.0	14.0	29.0	7.0	7.0
Min.	13.62	9.19	0.15	0.22	0.15	4.08	1.29	8.7	19.4	0.0	8.0	10.0	0.0	0.0

1) Nodule types: see in Fig. IX-1. n: number of data.

2) H+: loss of heating in Penfield tubes, H−: loss of heating at 110°C 3 hours. Concentrations of metal elements and H+ are normalized to 110°C dried sample and H− to air-dried ones.

3) Mineral amounts are listed as relative abundance. The abundances are comparable within one mineral but not significant to other minerals. T: Xray-intensity at 10 Å reflection, D: δ-MnO_2 calculated from those at 10 and 2.4 Å reflections, Q: quartz, Ph: phillipsite, Pc: plagioclase.

phases.

Relationship between chemical and mineral compositions

It has been noted that the compositions of minor metal elements in manganese nodules are usually correlated to those of major elements, Mn and Fe (CALVERT and PRICE, 1977; CRONAN, 1977), and are closely related to mineral composition (BURNS and FUERSTEAU, 1966; SOREM, 1977, USUI, 1979).

If the following assumptions are accepted, the inter-element relationships of these nodules are reasonably interpreted on mineralogical basis;

1) Manganese nodules consists of three extreme components of invariable chemical composition, 10 Å manganate phase, δ–MnO_2 phase and aluminosilicate minerals.
2) 10 Å manganate is stoichiometric transition metal(s)-manganate. The ratio of Ni plus Cu to Mn is constant.
3) δ–MnO_2 is cryptocrystalline mixture of manganese and iron oxides and contains no Cu or Ni. The ratio Mn to Fe is 1.0.
4) Amounts of the two ferromanganese components are independently variable; amounts of aluminosilicate fraction are also variable but do not exceeds around 20 wt.% as oxides.

Under these assumptions, plots for Mn, Fe, Cu plus Ni, Fe/Mn and intensity of at 10 Å reflection (Fig. XV–1A to 1J) are compatibly explainable. In these plots, solid symbols represent bottom gritty surface or rough surface nodules with dominant 10 Å manganate, and open symbols dominant δ–MnO_2. Major elements Mn and Fe are consequently weakly correlated and of scattered pattern (Fig. XV–1E). The plots of open and solid symbols fall in the characteristic region in the figure, which reflects the difference in chemical composition of two major mineral constituents.

It is deduced from the assumptions that ratio Fe/Mn is of linear dependence of ratio of amounts of the δ–MnO_2 phase to the sum of δ–MnO_2 and 10 Å manganate phases. Figures XV–1A and 1B represent the relationship of major elements and mineral composition. The ratio Fe/Mn is expected to vary proportionally to the relative amount of the δ–MnO_2 phase. The ratios, Mn/Fe and Mn/(Mn+Fe) often used may not have linear relationship to mineral amount.

The correlation plot of Cu plus Ni versus Mn concentrations shows a considerably dispersed pattern (correlation coefficient $r = +0.83$) and some (more than 10%) of manganese are not responsible to the concentration of Cu plus Ni (Fig. XV–1C). However, the correlation plot of Cu plus Ni versus 10 Å reflection intensity shows strong linear dependency of Cu plus Ni to 10 Å manganate abundance ($r = +0.92$), and the regression line cross the axes near the zero point (Fig. XV–1D). This is an evidence for mineralogical control of the minor metal elements.

It is reasonable on the assumptions that Cu plus Ni concentration is strongly and positively correlated with Fe/Mn (Fig. XV–1F). In Figure XV–1C, Cu plus Ni ceases around 15% Mn in Mn-axis. The amount of Mn less than around 15% is attributable to the δ–MnO_2 phase, while high concentration of Cu plus Ni and excess Mn is attributable to the 10 Å manganate and δ–MnO_2 phases. Likewise higher concentrations of Mn than 15 to 20% is attributable to both in Figure XV–1B.

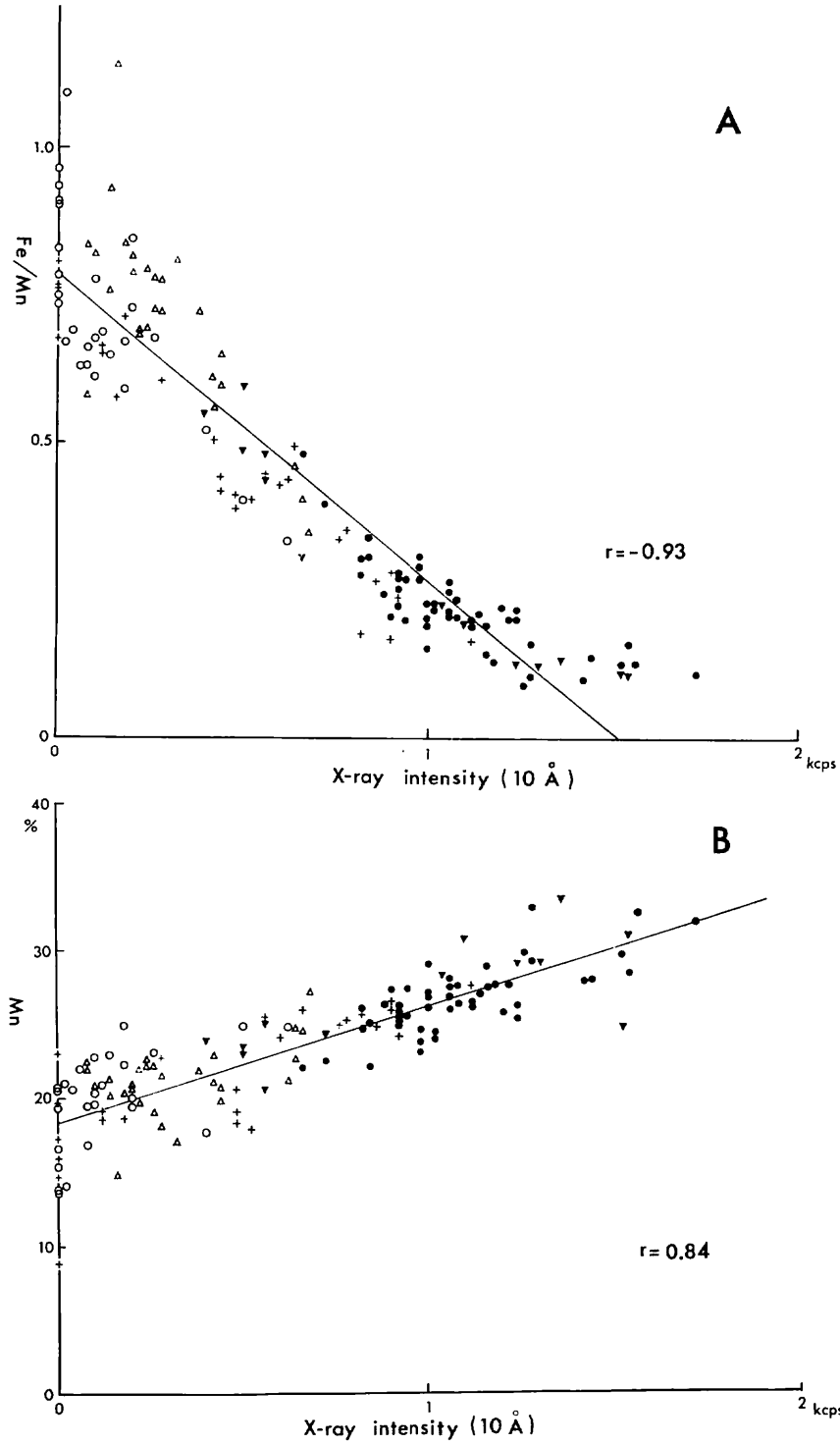
A
Fe/Mn
1.0
0.5
0
r=-0.93
0
1
2 kcps
X-ray intensity (10 Å)
B
%
40
30
20
10
0
Mn
r=0.84
0
1
2 kcps
X-ray intensity (10 Å)

Fig. XV-1 (1)

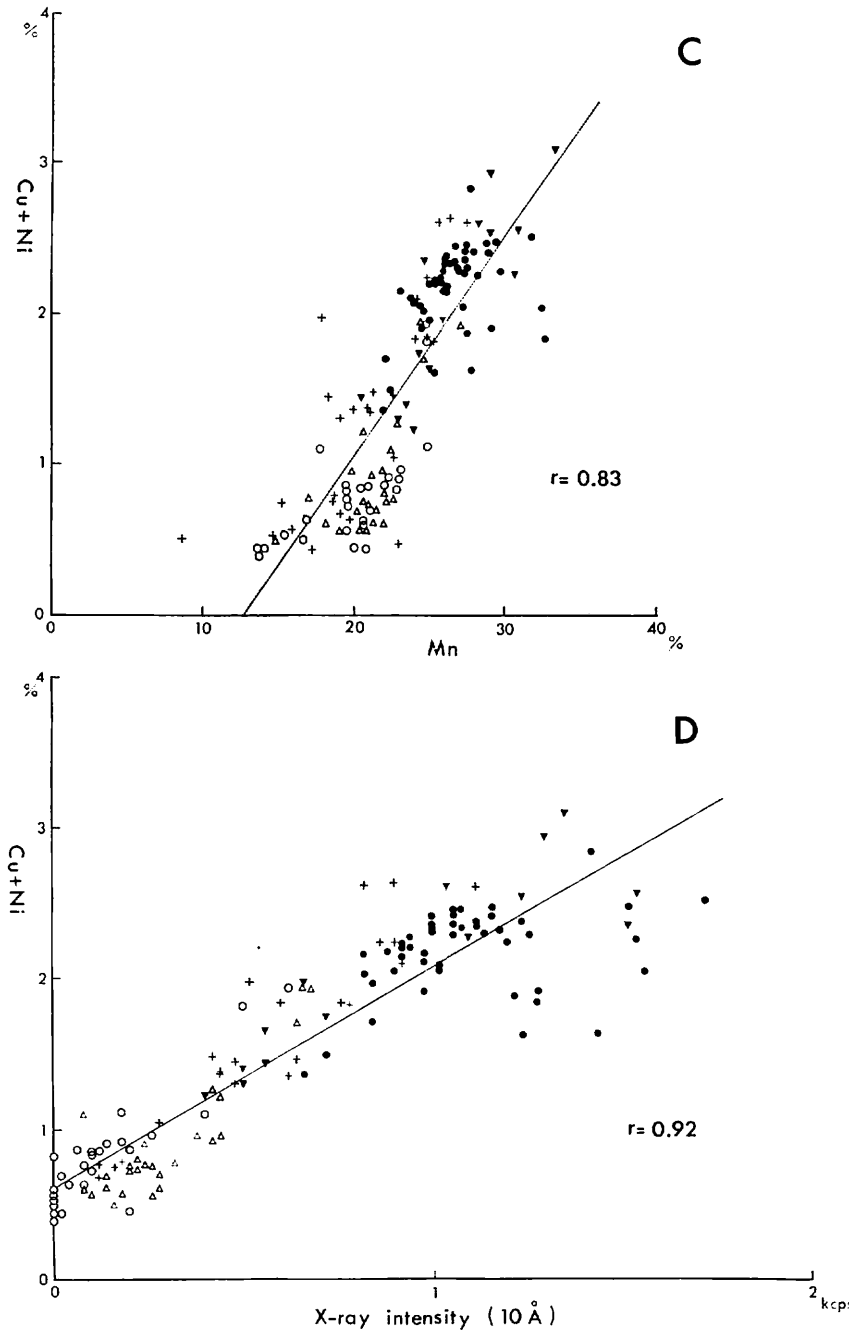

Fig. XV-1 (2)

Fig. XV–1 Correlation plots of chemical composition with mineralogical parameters. Symbols denote analysed parts in nodules. X-ray intensity is measured from peak height on diffractograms (full scale: 2 kcps), showing relative abundance of 10 Å manganate. The regression lines are drawn through all data points by means of the least square method assuming horizontal components have no error. r: correlation coefficient.

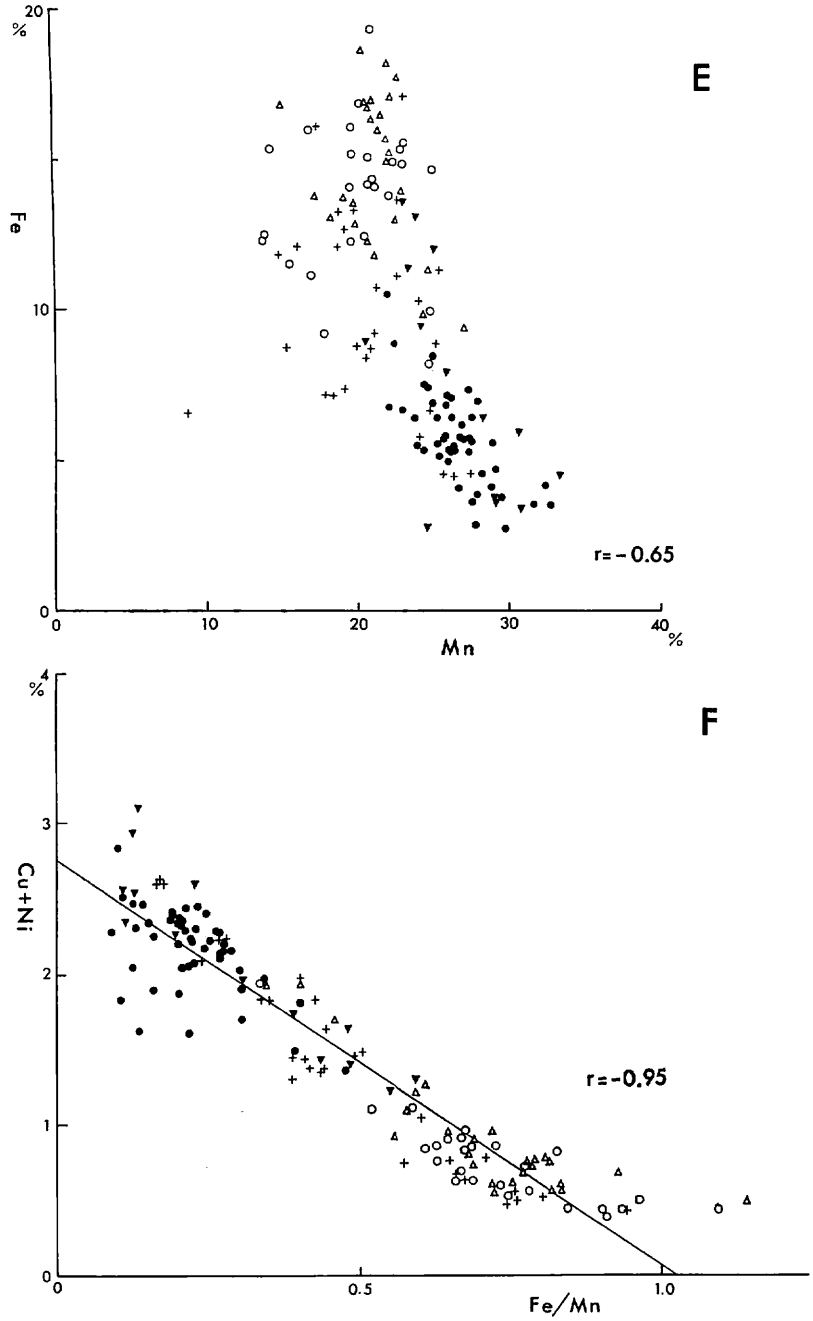

Fig. XV-1 (3)

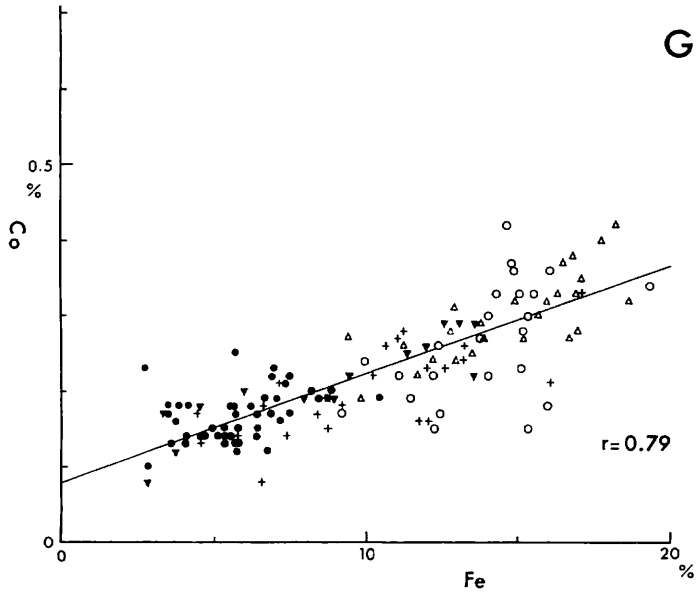

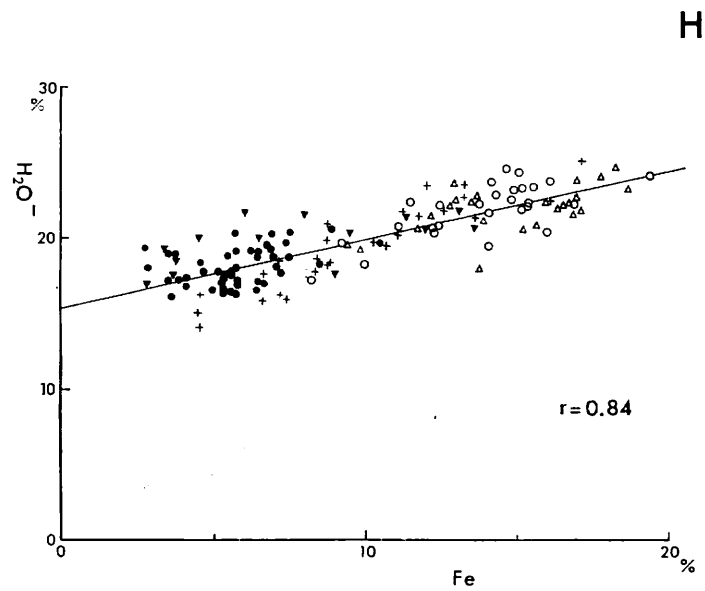

Fig. XV-1 (4)

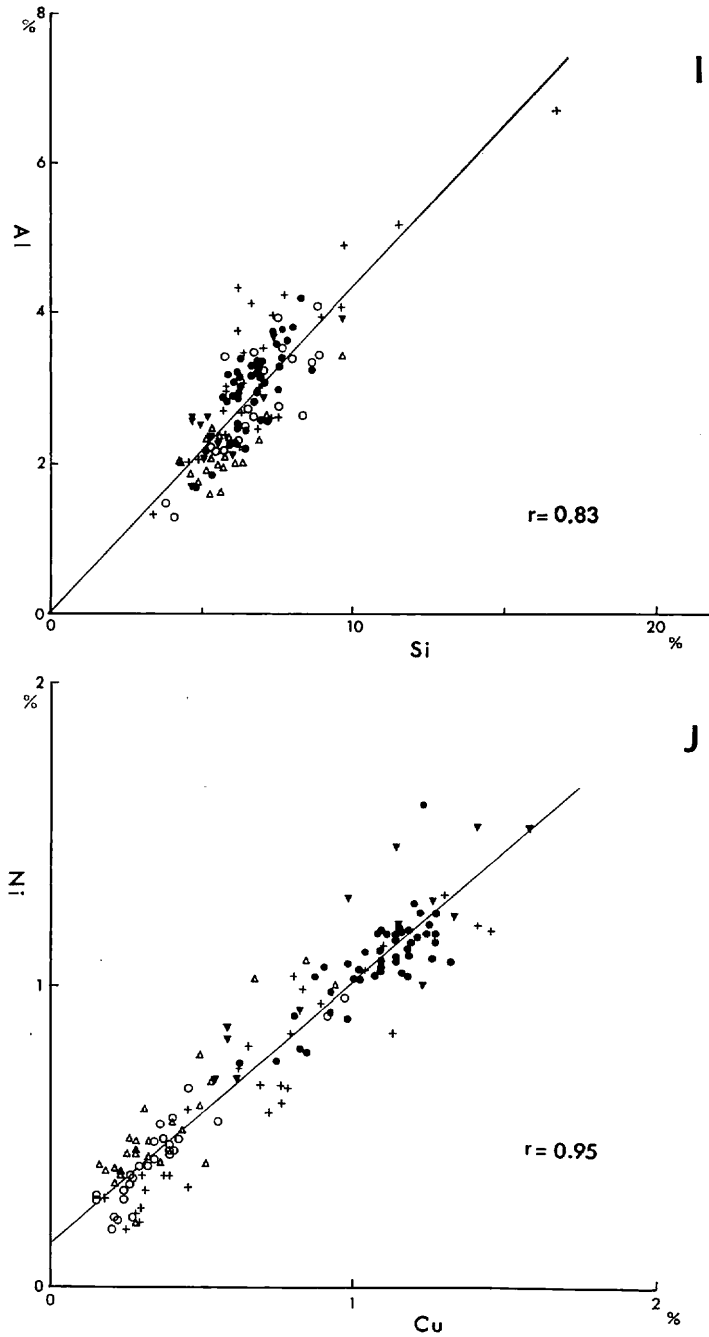

Fig. XV-1 (5)

Co in nodules has been considered to be incorporated to iron compounds substituting Fe^{3+} sites or in manganese compounds substituting Mn^{4+} (BURNS, 1976). Anyway it seems reasonable to attribute the concentration of Co to the δ–MnO_2 phase (Fig. XV–1G).

Water content (H_2O+) is not strongly correlated to Fe or other components (Fig. XV–1H). Water content (H_2O-) is well correlated to Fe concentrations, controlled by the physical characteristics of ferric hydroxides as noted by HALBACH and ÖZKARA (1979).

Deviations from the deduced trends are probably due to variability of minor aluminosilicate components and another irregularity in crystal chemistry of two minerals components.

Plot of Si versus Al show fairly good positive correlation, with the regression line crossing axes near the zero point (Fig. XV–1I). The mean of Si/Al atomic ratio of these nodule samples is around 2.3 ranging from 1.9 to 2.5. It is similar but slightly low as compared with reported ratios for marine phillipsites (2.4 to 2.8: BOLES, 1977). The correlation between Si and quartz is relatively weak ($r=0.52$). Quartz or amorphous silica such as biogenic tests may not be dominant component of silica in the manganese nodules. It is suggested that aluminosilicates e.g. phillipsite are the most important constituent for silica in manganese nodules of this area.

The strongest positive correlation ($r=+0.95$) in Figure XV–1J is not explainable simply by the variation of mineral abundance.

Table XV–3 shows correlation matrix for 15 components combining chemical composition with mineral composition. Figure XV–2 is the result of cluster analysis in which the correlation between groups were recalculated by simple arithmetic averaging. It reveals well-grouped three classes: 1) Mn–Cu–Ni and 10 Å manganate, 2) Fe–Co–$H_2O\pm$ and δ–MnO_2, and 3) Si–Al, phillipsite, plagioclase, montmorillonite and quartz. The correlation coefficients are generally negative between the three groups

Table XV-3 Correlation matrix for chemical and mineral analyses (n=145).

	Mn	Cu	Ni	T	Si	Al	Qtz	Ph	Pc	Mmt	Fe	Co	H−	H+	D*
Mn	1														
Cu	0.79	1													
Ni	0.86	0.95	1												
T	0.84	0.91	0.91	1											
Si	−0.38	0.00	−0.11	−0.10	1										
Al	−0.12	0.36	0.23	0.14	0.83	1									
Qtz	0.19	0.45	0.40	0.53	0.52	0.47	1								
Ph	−0.34	0.00	−0.15	−0.20	0.62	0.66	0.16	1							
Pc	−0.44	−0.18	−0.27	−0.24	−0.64	0.52	0.34	0.48	1						
Mmt	−0.25	−0.02	−0.04	−0.02	0.60	0.45	0.40	0.26	0.51	1					
Fe	−0.65	−0.91	−0.84	−0.89	−0.14	−0.42	−0.60	−0.09	−0.01	−0.15	1				
Co	−0.28	−0.65	−0.57	−0.62	−0.33	−0.51	−0.59	−0.14	−0.22	−0.26	0.79	1			
H−	−0.44	−0.79	−0.69	−0.72	−0.35	−0.61	−0.61	−0.24	−0.11	−0.18	0.84	0.76	1		
H+	−0.43	−0.43	−0.44	−0.48	−0.23	−0.25	−0.45	0.00	−0.07	−0.21	0.45	0.29	0.23	1	
D*	−0.81	−0.84	−0.86	−0.95	0.16	−0.08	−0.43	0.24	0.30	0.07	0.80	0.55	0.66	0.41	

Significance levels: coefficient $|r|>0.163$ at 95%, $|r|>0.213$ at 99%, and $|r|>0.315$ at 99.9%.

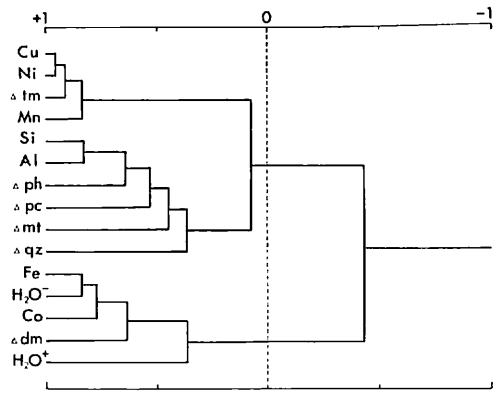

Fig. XV–2 Dendrogram drawn on the basis of cluster analysis using correlation coefficients as similarity parameters. Symbols with small triangle denote mineral abundances; tm: 10 Å manganate, dm: δ–MnO_2, ph: phillipsite, pc: plagioclase, mmt: montmorillonite, qz: quartz.

and positive within each group. The results are again in good accordance with the above-mentioned assumptions.

Figure XV–3 summarizes the relationship between morphology, chemistry and mineralogy. 10 Å manganate rich samples and δ–MnO_2 rich samples are clearly differentiated on the line combing the two extreme chemical compositions. The figure suggests a possibility of estimation of the concentration of Cu plus Ni from Mn and Fe concentrations. The multiple regression analysis estimates the coefficients of the following equation:

$$Z = a(\mathrm{Mn}) + b(\mathrm{Fe}) + c \quad (a = +0.077;\ b = -0.099;\ c = +0.70)$$

where Z is the estimated concentration of Cu plus Ni, (Mn) and (Fe) are analysed concentrations in wt.%. The multiple correlation coefficient in the regression is +0.95. The results strongly suggest significance of the estimation of Cu plus Ni from Mn and Fe concentrations.

Bulk nodule compositions consequently seem to fall within the range combing two constituents which are of extreme chemical compositions.

Local variations on detailed survey lines

As stated in the previous section, the common chemical characteristics to manganese nodules from all of detailed survey lines is that the mineral composition principally determines their chemical composition and surface features. Internal structure and microstructure of nodules are also closely related to mineral composition as reported by Usui (Chapter XIV in this cruise report). Local variations of several parameters of chemistry and mineralogy are shown in Figure XV–4.

The fluctuation of silica and alumina contents is relatively small along the survey lines. Distinct patterns of variation are not recognized with nodule morphology or manganese mineral composition, except for slightly high concentrations of Si and Al in internal older nodules as a result of incorporation of zeolitic rock nuclei. In con-

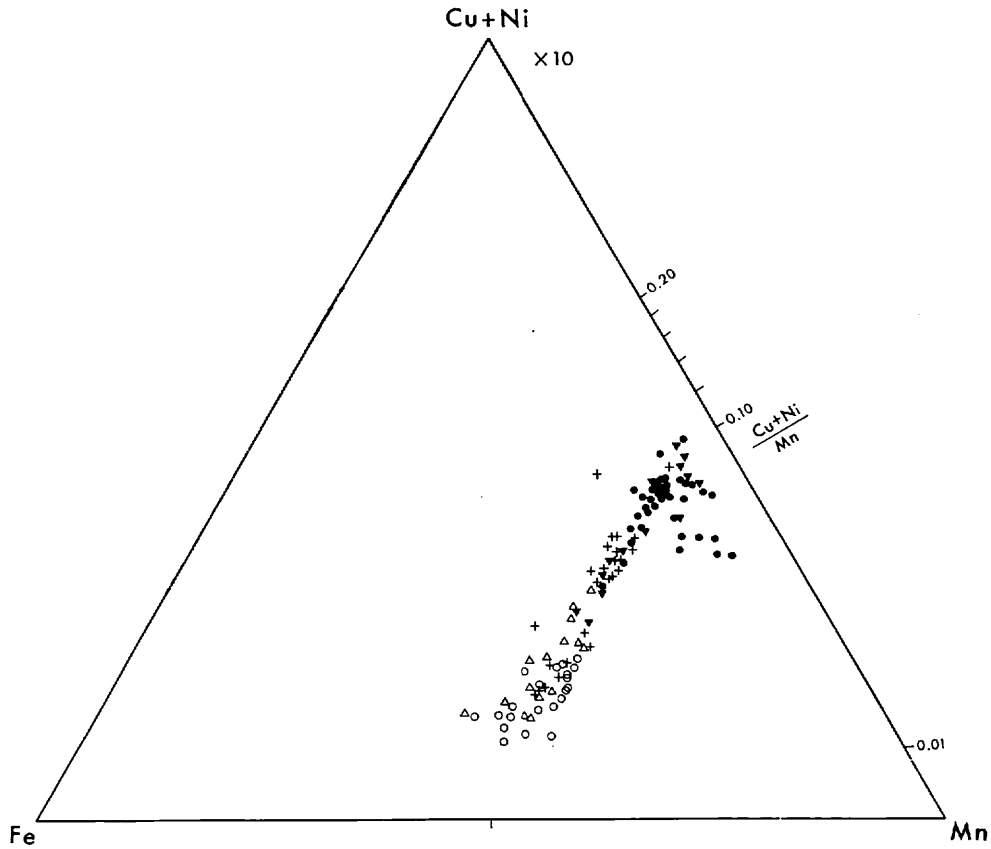

NODULE TYPE AND ANALYZED PART

△ top or outer layer of s, s+s·r, and s+r

▼ bottom of s+s·r, s+r, and s·r+r

○ internal older nodules of s, s+s·r, and s+r

● r and s·r+r (whole nodule or outer layer)

+ other samples (inner part of r, whole of s+r etc.)

Fig. XV–3 Plot of ratios Mn/Fe/(Cu+Ni)×10. Open symbols related to 10 Å manganate and solid symbols related to δ–MnO_2 are well grouped, and the pattern of scattering suggests a possible linear regression.

trast, the compositions of major elements, Mn and Fe, greatly vary with nodule morphology and internal structure. Along five survey lines, pattern of variation of nodule internal structure is similar. Rough-surface nodules (e. g., type r) composed of entirely concentric 10 Å manganate layers show little variation in chemical composition in spite of their wide localities extending several tens kilometers. The chemical composition of internal older nodules is also fairly constant, and no clear variation with locality is observed.

For example, the chemical characteristics of r-type nodules from the northern

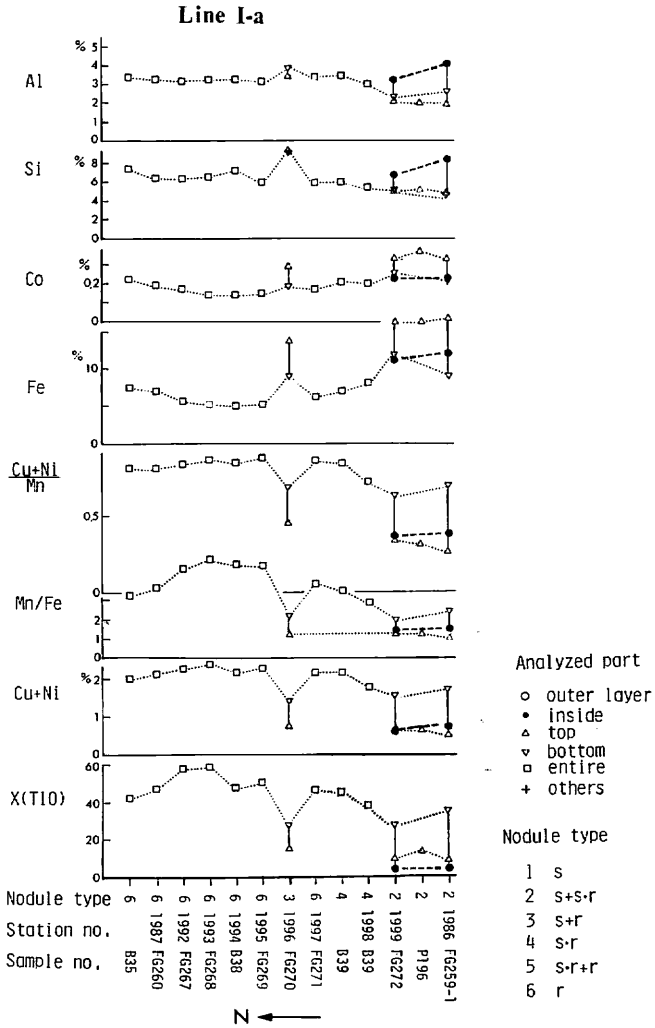

Fig. XV-4 (1)

Fig. XV-4 Line profiles of chemical and mineralogical characteristics of manganese nodules. Corresponding samples are combined by dotted or dashed lines. X(T10) is the X-ray intensity at 10 Å determined in the same measurement conditions in percent of full scale of 2 kcps.

stations of St. 2037 on the line II–c is relatively invariable, though the actual amount of 10 Å manganate considerably varies. Cu plus Ni amounts around 2.0% and Mn/Fe exceeds 4. On the other hand, smooth-surface nodules are composed of internal older nodules and surrounding layers. Cu plus Ni is less than 0.5% and Mn/Fe is around 1.0 in internal nodules. Surrounding layers, tops and bottoms are more variable in composition. It seems that outermost rough 10 Å manganate layers are ubiquitously but variably distributed on most nodule surfaces, while the area

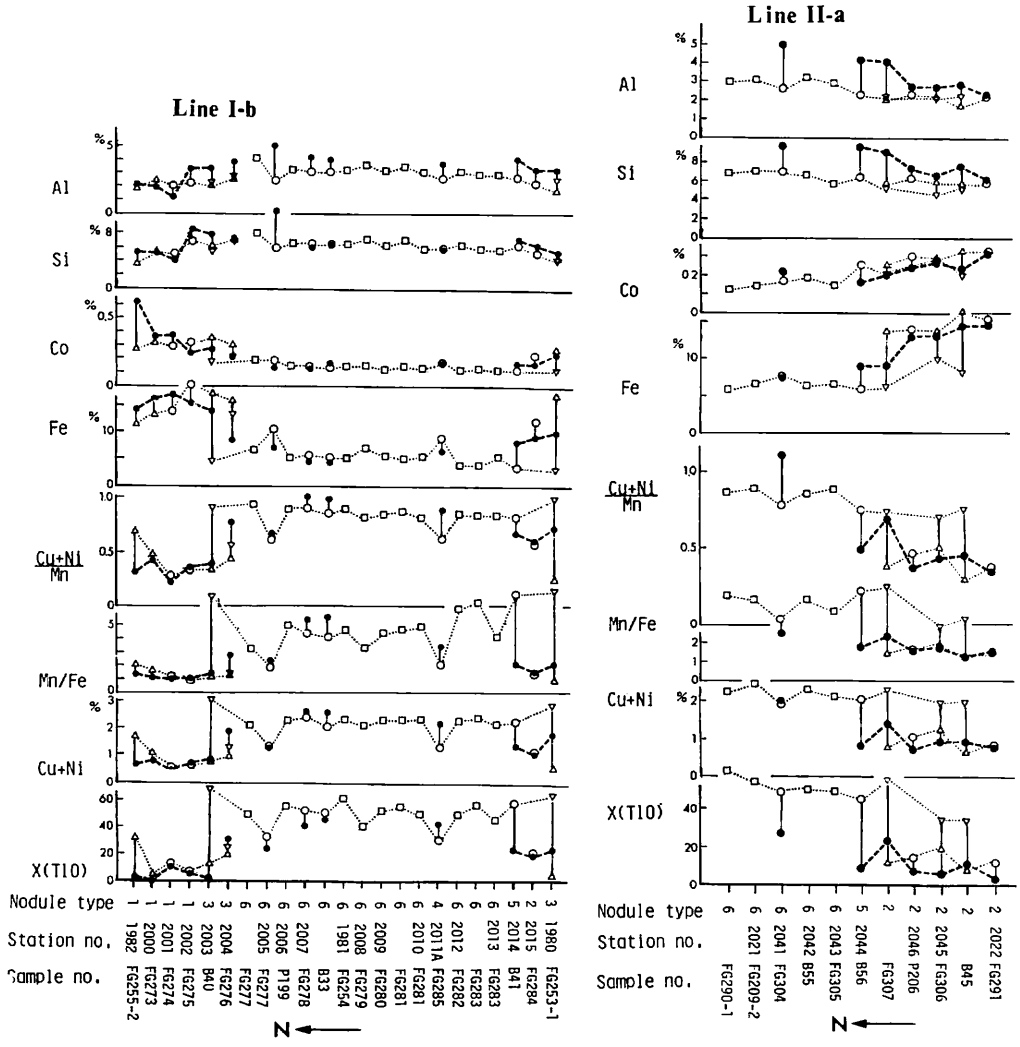

Fig. XV-4 (2)

of distribution of the δ–MnO_2 phase is limited.

It is concluded that the variability of bulk chemistry of nodule is principally determined by the variability of relative mineral abundance in nodules and mode of development in each nodule. It is because the chemical composition of the two mineral is significantly invariable despite variable mode of growth in each nodule or nodule locality.

It is suggested that the controlling factors of local variability in morphology and chemical composition are the past and present marine conditions in which either mineral constituent is preferentially deposited.

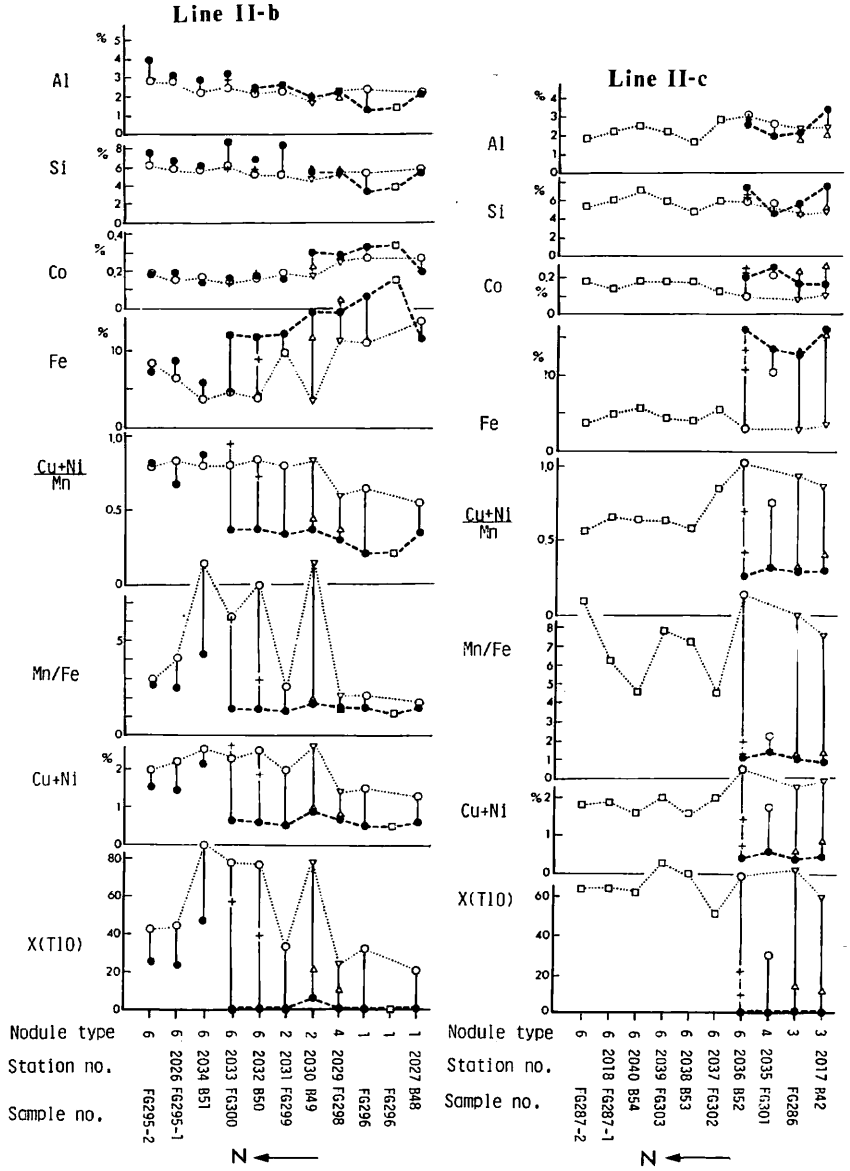

Fig. XV-4 (3)

References

ANDREWS, J. E. and FRIEDRICH, H. W. (1979) Distribution patterns of manganese nodule deposits in the Northeast Equatorial Pacific. *Marine Mining*, vol. 2, no. 1/2, p. 1–43.

BOLES, J. R. (1977) Zeolites in deep-sea sediments. *In* MUMPTON, F. A. (ed.) *Mineralogy and Geology of Natural Zeolites*. Mineral. Soc. Am. Short Course Notes, vol. 4, p. 137–163.

BURNS, R. G. (1976) The uptake of cobalt into ferromanganese nodules, soils, and synthetic manganese (IV) oxides. *Geochim. Cosmochim. Acta*, vol. 40, p. 95–102.

BURNS, R. G. and FUERSTENAU, D. W. (1966) Electron probe determination of inter-element relationships in manganese nodule. *Am. Mineral.* vol. 51, p. 895–902.

CALVERT, S. E. and PRICE, N. B. (1977) Geochemical variation in ferromanganese nodules and associated sediments from the Pacific Ocean. *Marine Chemistry*, vol. 5, p. 43–74.

CRONAN, D. S. (1977) Deep-sea nodules: Distribution and geochemistry. *In* GLASBY, G. P. (ed.) *Marine Manganese Deposits.* Elsevier Oceanography Series, 15, p. 11–44.

FRAZER, J. Z. and WILSON, L. L. (1979) *Manganese nodule deposits in the Indian Ocean.* SIO Reference Ser. 79–18, pp. 71.

FUJINUKI, T., MOCHIZUKI, T., and MORITANI, T. (1977) Chemical composition of manganese nodules. *Geol. Surv. Japan Cruise Rept.*, no. 8, p. 162–171.

HALBACH, P. and ÖZKARA, M. (1979) Morphological and geochemical classification of deep-sea ferromanganese nodules and its genetical interpretation. *In* LALOU, C. (*ed.*) *La Genèse des Nodules de Manganèse*, C. N. R. S. Rept., no. 289, p. 77–88.

HORN, D. R., HORN, B. M., and DELACH, M. N. (1972) Distribution of ferromanganese deposits in the world ocean. *In* HORN, D. R. (*ed.*) *Ferromanganese Deposits on the Ocean Floor.* N. S. F., Washington, D.C., p. 9–17.

MIZUNO, A. (1981) Regional and local variabilities of manganese nodules in the Central Pacific. *Geol. Surv. Japan Cruise Report*, no. 15, p. 281–296.

RAAB, W. (1972) Physical and chemical features of Pacific deep sea manganese nodules and their implications to the genesis of nodules. *In* HORN, D. R. (*ed.*) *Ferromanganese Deposits on the Ocean Floor.* N. S. F., Washington D.C., p. 31–49.

SOREM, R. K. and FEWKS, R. H. (1977) Internal characteristics of manganese nodules. *In* GLASBY, G. P. (*ed.*) *Marine Manganese Deposits.* Elsevier Oceanography Series, 15, p. 147–183.

TERASHIMA, S. (1978) Atomic absorption analysis of Mn, Fe, Cu, Ni, Co, Pb, Zn, Si, Al, Ca, Mg, Na, K, Ti and Sr in manganese nodules. *Bull. Geol. Surv. Japan*, vol. 29, p. 401–411.

USUI, A. (1979) Minerals, metal contents, and mechanism of formation of manganese nodules from the Central Pacific Basin (GH76–1 and GH77–1 areas). *In* BISCHOFF, J. L. and PIPER, D. Z. (*eds.*) *Marine Geology and Oceanography of the Pacific Manganese Nodule Province.* Marine Sci. Ser, vol. 9. Plenum Publ. Co., p. 651–679.

USUI, A., TAKENOUCHI, S. and SHOJI, T. (1978) Mineralogy of deep sea manganese nodules and synthesis of manganese oxides: Implications to genesis and geochemistry. *Mining Geology*, vol. 28, p. 405–420 (in Japanese with English abstract).